Stabilization and Acidic Dissolution Mechanism of Single-Crystalline ZnO(0001) Surfaces in Electrolytes Studied by In-Situ AFM Imaging and Ex-Situ LEED

Markus Valtiner,[†] Sergiy Borodin,[‡] and Guido Grundmeier*[,†,§]

Christian Doppler Laboratory for Polymer/Metal Interfaces at the Max-Planck-Institut für Eisenforschung, Max-Planck-Strasse 1, D-40237 Düsseldorf, Germany, and Technical and Macromolecular Chemistry, Department of Chemistry, University of Paderborn, D-33098 Paderborn, Germany

Received November 30, 2007. Revised Manuscript Received January 27, 2008

A combined approach of pH-dependent in-situ AFM topography and ex-situ LEED studies of the stability and dissolution of single-crystalline ZnO(0001)−Zn surfaces in aqueous media is presented. Hydroxide-stabilized and single-crystalline ZnO(0001)−Zn surfaces turned out to be stable within a wide pH range between 11 and 4 around the point of zero charge of $pH_{PZC} = 8.7 \pm 0.2$. Hydroxide stabilization turned out to be a very effective stabilization mechanism for polar oxide surfaces in electrolyte solutions. The dissolution of the oxide surface started at an acidic pH level of 5.5 and occurred selectively at the pre-existing step edges, which consist of nonpolar surfaces. In comparison, the oxide dissolution along the ZnO(0001) direction proved to be effectively inhibited above a pH value of 3.8. On the basis of these microscopic observations, the mechanistic understanding of the acidic dissolution process of ZnO could be supported. Moreover, both the in-situ AFM and the ex-situ LEED studies showed that the stabilization mechanism of the ZnO(0001) surfaces changes in acidic electrolytes. At pH values below 3.8, the hydroxide-stabilized surface is destabilized by dissolution of the well-ordered $\sqrt{3}\cdot\sqrt{3}\cdot$ R30 hydroxide ad-layer as proven by LEED. Restabilization occurs and leads to the formation of triangular nanoterraces with a specific edge termination. However, below pH 4 the surface structure of the crystal itself is ill-defined on the macroscopic scale because preferable etching along crystal defects as dislocations into the bulk oxide results in very deep hexagonal etching pits.

Introduction

Almost all functional metals, which are of high industrial and technological importance, are covered by a native oxide film. The stability of these oxide films determines the corrosion resistance of materials as these thin films passivate and thereby protect the surface from further oxidation.[1,2] Moreover, molecular adhesion forces at interfaces between organic coatings or adhesives and engineering metals are governed by the physisorption or chemisorption of macromolecules or adhesion-promoting additives on these passive film surfaces.[3] In this context, the stability of passivating oxides is of great interest for effective corrosion protection;[4] an understanding of the surface chemistry on the molecular level is important for polymer adhesion on oxide-covered metal substrates.[5] In particular, because zinc is a widely used metallic coating for steel,[6] the stability of passivating ZnO films is of high technical interest. Because corrosion reactions such as the cathodic delamination of organic coatings or crevice corrosion are accompanied by a change in the pH at the interface[3,7,8] it is necessary to understand the stability, surface chemistry and dissolution behavior of ZnO as a function of pH.

However, studying native oxide films formed on metal substrates is experimentally very challenging, and the choice of the model system is extremely important in enabling a better mechanistic understanding of the behavior of zinc oxides in electrolytes. The difficulties of investigating native oxide films on metal substrates in electrolytes are complex in both experiment and theory. First, oxide layers on metals have an inhomogeneous composition, which is the result of the growth process on the metal substrate leading to vertical stochiometry gradients in many passive films on metals.[1,2] Second, the dissolution of an oxide on a metal substrate is always accompanied by the simultaneous growth of the oxide on the metal. Ion and electron transport phenomena through the oxide and interfacial oxidation reactions accompany the dissolution of the oxide. Furthermore, native oxide layers on metal substrates are usually amorphous, and surface reactions cannot be investigated on a well-defined basis.

In contrast, using single-crystalline bulk oxides allows a defined study of oxides decoupled from any oxidative interfacial reaction. Moreover, using single-crystalline oxides enables the interpretation of data on a much better basis because the crystallographic orientation provides a solid idea of the surface structure. Another important aspect is that using single-crystalline substrates also allows for experimental studies, which are in close agreement with the inevitable idealizations of ab initio simulation approaches because a combined approach, or even the bridging of theory and experiment, is extremely important for a detailed understanding of interfacial processes on the molecular level.

* Corresponding author. Tel: +49/5251/60-3646. E-mail: g.grundmeier@tc.uni-paderborn.de.

[†] Christian Doppler Laboratory for Polymer/Metal Interfaces at the Max-Planck-Institut für Eisenforschung.

[‡] Max-Planck-Institut für Eisenforschung.

[§] University of Paderborn.

(1) Marcus, P.; Oudar, J. *Corrosion Mechanisms in Theory and Practice*; Marcel Dekker: New York, 1995.

(2) Zhang, X. G. *Corrosion and Electrochemistry of Zinc*; Plenum Press: New York, 1996; pp 65–91.

(3) Grundmeier, G.; Schmidt, W.; Stratmann, M. *Electrochim. Acta* **2000**, *45*, 2515–2533.

(4) Grundmeier, G.; Reinartz, C.; Rohwerder, M.; Stratmann, M. *Electrochim. Acta* **1998**, *43*, 165–174.

(5) Grundmeier, G.; Stratmann, M. *Ann. Rev. Mater. Res.* **2005**, *35*, 571–615.

(6) Faderl, J.; Strutzenberger, J.; Wolpers, M.; Fischer, W. *Stahl Eisen* **2001**, *121*, 73–79.

(7) Leng, A.; Streckel, H.; Stratmann, M. *Corros. Sci.* **1999**, *41*, 579–597.

(8) Furbeth, W.; Stratmann, M. *Corros. Sci.* **2001**, *43*, 207–227.

10.1021/la7037697 CCC: $40.75
Published on Web 04/26/2008

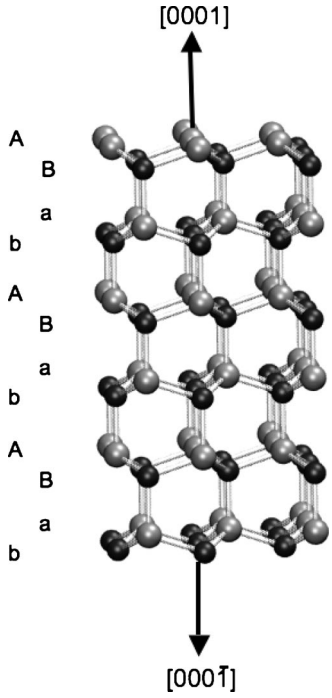

Figure 1. Side view of the polar Zn-terminated [0001] and O-terminated [000$\bar{1}$] ZnO surfaces.

The herein investigated single-crystalline ZnO(0001)−Zn surfaces have been extensively studied under UHV conditions within the last few decades.[9–11] In contrast, the literature on well-defined crystalline ZnO(0001)−Zn surfaces under ambient conditions and in electrolyte solutions is not very comprehensive.[12–16] In principle, the ZnO(0001)−Zn surface was expected to be unstable because of its polar nature. Along the *c* direction, the ZnO crystal consists of an alternating sequence of hexagonally closed-packed layers of Zn^{2+} and O^{2-} ions (Figure 1). This leads to a dipole moment perpendicular to these planes. Within the bulk, these dipole moments completely compensate for each other. A perfect surface cut normal to the *c* axis of the ZnO leads to ZnO(0001)−Zn surfaces on one side of the slab and ZnO(000$\bar{1}$)−O surfaces on the other side of the slab (Figure 1) and the dipole moment on the surface cannot be compensated for. The resulting polar surfaces are called tasker-type 3 surfaces and are expected to be unstable because of the dipole moment normal to the surface;[17] consequently, reconstruction was expected. The interesting feature of Zn-terminated ZnO(0001)−Zn surfaces was that no reconstruction has been observed, which was discussed quite controversially in the literature. Arguing with an ionic model, it is clear that the perfect Zn-terminated surface itself would be positively charged as a result of the nature of the polar ZnO(0001)−Zn surface. The surface Zn^{2+} ions have three oxide ions as nearest neighbors. Thus, formally ½e^- per unit cell area is necessary to compensate for the positive charge and quench the dipole moment normal to the surface. (1) Electron transfer from the O-terminated to the Zn-terminated side, (2) the formation of ¼ML Zn and O vacancies on the respective side, and (3) adsorption of ½ML of hydrogen and hydroxides on the respective sides were discussed as potential stabilization mechanisms. Experimentally, stabilization by the formation of Zn vacancies[9,10] via a high density of steps (oxygen-terminated) of UHV-prepared surfaces and hydroxide stabilization[18,19] of wet chemically prepared surfaces (alkaline etching) were proven to be effective stabilization mechanisms for ZnO(0001)−Zn surfaces.

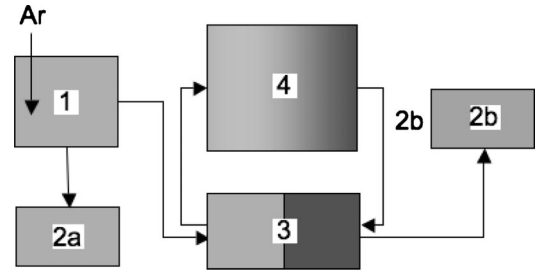

Figure 2. Scheme of the used setup for in-situ AFM studies of nonequilibrium reactions. (1) Base solution purged with Ar, (2a,b) ex-situ pH measurement with micro pH electrodes, (3) syringe pump, and (4) AFM cell.

In this work, the stability and dissolution behavior of hydroxide-stabilized ZnO(0001)−Zn surfaces within electrolyte solutions was investigated by a combined approach of in-situ AFM studies and ex-situ LEED studies. In-situ AFM studies are a very suitable method for understanding the evolution of surface structures in electrolytes and are widely used in the field of geochemistry.[20–24] The combined approach with ex-situ LEED allowed the investigation of the stability of single-crystalline ZnO(0001)−Zn surfaces in electrolyte solutions with regard to the mechanistic understanding of oxide dissolution and stability.

Experimental Section

Chemicals and Sample Preparation. All chemicals were of p.a. grade (analytical reagent grade) and were used as supplied without any further purification. The water used for the experiments was deionized (18.2 MΩ cm^{-1} resistivity) with a Purelab Plus UV (USF) filtration system. All glass and Teflon equipment was cleaned with Piranha solution (H_2SO_4(conc.)/H_2O_2(30%) = 1:1), all other equipment was cleaned using a standard RCA-I cleaning.[25] (***Caution!*** *Piranha solution can react violently with organic materials and should be handled with extreme caution.*) The hydrothermally grown ZnO single crystals with ZnO(0001)−Zn polished faces (<0.1° accuracy) were obtained from MaTecK GmbH (Juelich, Germany). The size of the single crystals was 20 mm × 20 mm × 0.5 mm for the AFM investigations and 8 mm × 8 mm × 0.5 mm for the LEED investigations. ZnO(0001)−Zn−OH surfaces that are stabilized by hydroxides were prepared with slight modifications according to the literature (Technique B in[18]). The heat treatment of the crystals was done in an aluminum oxide tube furnace with horizontal setup[26] in a pure oxygen atmosphere containing 4% water vapor.

(9) Dulub, O.; Diebold, U.; Kresse, G. *Phys. Rev. Lett.* **2003**, *90*, 000.
(10) Dulub, O.; Boatner, L. A.; Diebold, U. *Surf. Sci.* **2002**, *519*, 201–217.
(11) Woll, C. *Prog. Surf. Sci.* **2007**, *82*, 55–120.
(12) Gerischer, H.; Sorg, N. *Electrochim. Acta* **1992**, *37*, 827–835.
(13) Gerischer, H.; Sorg, N. *Werkst. Korros.* **1991**, *42*, 149–157.
(14) Inukai, J.; Ito, K.; Itaya, K. *Electrochemistry* **1999**, *67*, 1126–1128.
(15) Deren, J.; Nowok, J. *Rocz. Chem.* **1972**, *46*, 2361–2364.
(16) Hamann, T. W.; Gstrein, F.; Brunschwig, B. S.; Lewis, N. S. *J. Am. Chem. Soc.* **2005**, *127*, 7815–7824.
(17) Tasker, P. W. *J. Phys. C* **1979**, *12*, 4977–4984.
(18) Valtiner, M.; Borodin, S.; Grundmeier, G. *Phys. Chem. Chem. Phys.* **2007**, *9*, 2297–2436.
(19) Valtiner, M.; Grundmeier, G. In *Zinc Oxide and Related Materials*; Norton, D. P., Jagadish, C., Buyanova, I., Yi, G.-C., Eds.; Materials Research Society Symposia Proceedings; Materials Research Society: Warrendale, PA, 2007; Vol. *1035E.*
(20) Kuwahara, Y. *Am. Mineral.* **2006**, *91*, 1142–1149.
(21) Stumm, W. *Colloids Surf., A* **1997**, *120*, 143–166.
(22) Biber, M. V.; Afonso, M. D.; Stumm, W. *Geochim. Cosmochim. Acta* **1994**, *58*, 1999–2010.
(23) Hillner, P. E.; Gratz, A. J.; Manne, S.; Hansma, P. K. *Geology* **1992**, *20*, 359–362.
(24) Gratz, A. J.; Manne, S.; Hansma, P. K. *Science* **1991**, *251*, 1343–1346.
(25) Kern, W.; Puotinen; D, A. *RCA Rev.* **1970**, *31*, 187–206.
(26) Asteman, H.; Svensson, J. E.; Johansson, L. G.; Norell, M. *Oxid. Met.* **1999**, *52*, 95–111.

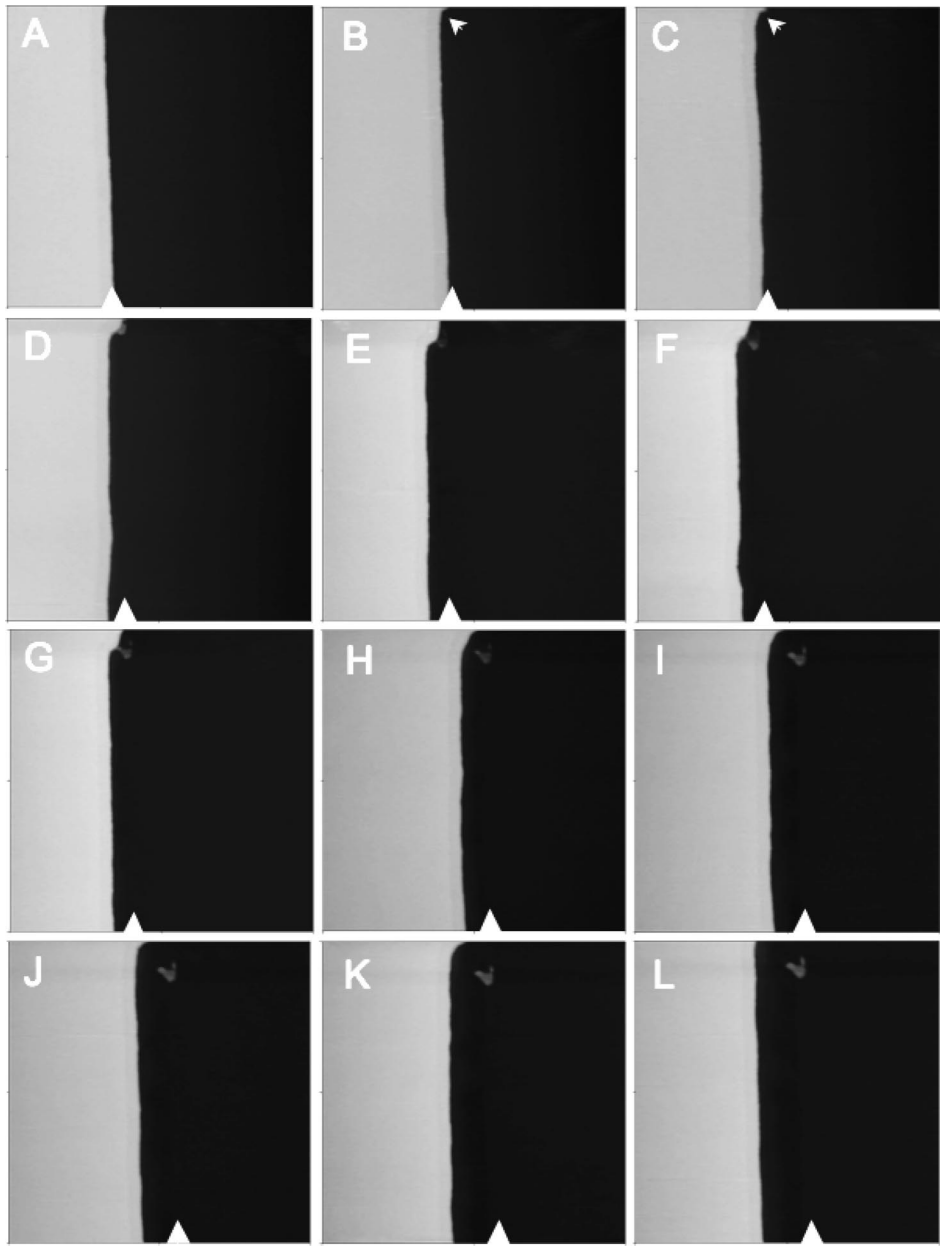

Figure 3. Dissolution behavior of the ZnO(0001)−Zn surfaces from pH 11 to 4. Scan size for all topography images was 1 μm × 1 μm. The step height is 4.8 nm. An appearing insoluble impurity can be used as good guidance for the observation and also ensures that no drift of the system is misinterpreted as a proceeding dissolution of an edge. The drawn markers should highlight the dissolution process. (A) Representative scan of the topography between pH 11 and 6 where no significant changes could be detected. (B) Scan after switching to pH 5.5 and (C) 20 min later. The drawn arrows indicate where the insoluble impurity will appear; in these scans, it is already slightly pronounced. Topography scans at pH 4.8 (D) after switching the pH, (E) 10 min later, and (F) 20 min later are displayed. Topography scans (G) after switching to pH 4.4 and (H) 10 min and (I) 20 min later. Topography after switching to pH 4.0 (J) 10 min and (K) and 20 min later. The images clearly show that the dissolution process starts and proceeds at preexisting edges.

Preparation of Solutions. For the experiments, all 1 mM solutions were prepared by diluting titrated base solutions. The base solutions of NaOH (0.2 mol/L) and $HClO_4$ (0.01 mol/L) were purchased from Sigma-Aldrich as eluent concentrates for ion chromatography. The pH was adjusted to between 11.0 and 3.0 using 1 mM NaOH/$HClO_4$, respectively, in a 1 mM base electrolyte of $NaClO_4$. This leads to a constant ionic strength. Additionally, the electrolyte was purged with argon for all measurements to avoid any effects (such as a pH shift and interfacial reactions) due to CO_2 contamination. The pH values were measured in fractions that were taken out of a stock solution in order to prevent any contaminating ions from making contact with the pH electrode (e.g., chlorides). Perchlorate was chosen as the anion because it does not promote the dissolution process by any surface complexation,[12,13] and this article focuses on the effects of pH ($H_3O^+/OH^-/H_2O$).

LEED. LEED measurements were performed at close-to-normal electron incidence with emission energies from 20 to 120 eV. The measurements were performed in an UHV system with a base pressure of 1×10^{-10} mbar.

AFM Investigations. AFM topography experiments were performed on a JPK NanoWizard AFM (JPK Instruments AG, Berlin, Germany) equipped with a custom-made liquid cell (material: PEEK; 500–700 μL liquid volume) providing the possibility to change the electrolyte in situ. Because we were investigating the dissolution of ZnO crystals, the measurements were made with a constant flow of 500 μL/min in order to prevent the equilibration of the dissolution process. This is necessary because the dissolution of the oxide consumes H_3O^+. With constant flow it is ensured that the H_3O^+ level and therefore the pH are stable at the adjusted values. A syringe pump (Micromechatronics AG, Germany) was used for that purpose.

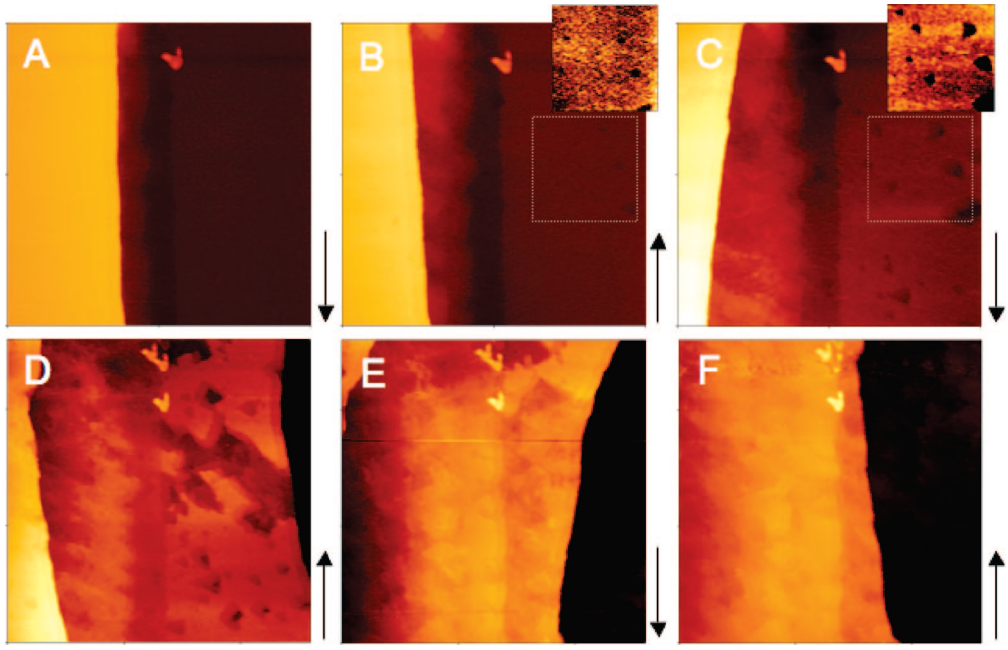

Figure 4. Evolution of the ZnO(0001)−Zn surface topography due to switching the pH from 4.0 to 3.6. The step height is still 4.8 nm. The insoluble impurities are a good guide for the eye. The scan size for topography images (A−C) was 1 μm × 1 μm. As the dissolution front was running out of the image, the scan size was enlarged to 1.2 μm × 1.2 μm for D and E. The arrows indicate the scan direction. (A) The scan directly after changing the pH of the base solution from 4.0 to 3.6, which corresponded to a pH of 3.9 in the electrolyte fraction that was collected after the cell. The dissolution started to proceed immediately with a higher speed as can be seen in the next scan (B) that was finished 3 min later. The pH of the collected fraction after the scan was 3.8. The small inlet clearly shows that the first pits are forming on the plateaux. The next scans (C−F) show the evolution (+3 min per scan) of the surface structure at the final pH of 3.6. The inlet in C shows that the initial pits are growing in the $x-y$ direction.

The pH values were measured (1) as fractions of the stock solution that was pumped through the cell, and (2) behind the cell 500 μL fractions were collected and measured to ensure that the desired pH value was adjusted within the cell as well. We explicitly avoided measuring the pH value with a micro pH electrode inside the cell (which would also be possible) because such an analysis could introduce contaminants such as chloride ions that are likely to affect the dissolution behavior.[12,13] A general flowchart of the setup is shown in Figure 2.

Furthermore, the AFM system is equipped with a homemade noise protection system that enables conditions for imaging with a noise level of ~1 Å. All images were recorded in contact mode using silicon sensors (CONTR obtained from NanoWorld, typical tip radius of <10 nm). The experiments were performed in constant force mode with a force of ~5–10 nN. The z piezo of the AFM was calibrated using a 1D array of rectangular SiO_2 steps with a height of 18.6 nm. The xy piezos were internally calibrated with integrated capacitive position sensors. All AFM measurements were analyzed using the SPIP software of the image metrology group and the implemented JPK software.

Results and Discussion

Stability and Dissolution on ZnO(0001)−Zn Surfaces: In-Situ AFM Studies Model surfaces were prepared according to procedure B as described in the literature.[18] Characteristically, these single-crystalline surfaces feature very large atomically flat plateaus in the micrometer range. The step heights are typically between 4 to 10 nm. Figures 3−5 show pH-dependent topography evolution occurring on this type of surface as studied by means of in-situ AFM without changing the imaging area. The inspection of this and other sequences revealed several consistent qualitative and quantitative results as discussed in the following section.

In-situ topography imaging was always started at pH 11 where no dissolution was expected;[12,13] the pH values were kept constant at certain pH steps for at least 2 h in order to be able to detect the slightest changes in topography. However, we were not able to detect any significant changes in topography within the pH range of 11 to 5.5, as can be seen in Figure 3a. In one experiment, the pH was kept at 6 for 12 h. Even for this extended time range, no significant change in surface topography could be detected.

Starting at a pH value of 5.5, surface dissolution was detected only at pre-existing steps in the structure as can be seen in Figure 3b,c. A further lowering of the pH values resulted in dissolution proceeding along the step edges as can be seen clearly in Figure 3d−l. The dissolution rate noticeably increases with decreasing pH values but remained slow in comparison to the rate at pH values below 4. Below pH 4, the dissolution rate appeared to increase significantly (Figure 4a−c). Changes could not be detected within the time scale of one scan anymore. This led to a tilt of the edge in the analyzed topographic images. We did not analyze the kinetics of the dissolution quantitatively because more accurate techniques are available to study the kinetics. For ZnO(0001)−Zn surfaces (even though pretreated differently), this was investigated by measuring the electrochemical dissolution current.[12,13] According to the literature, no dissolution current was detected between pH 12 and 5; dissolution currents could be measured starting at pH 5 and increased linearly on a logarithmic scale with decreasing pH. Within our investigation, we found that dissolution was first detected starting at pH 5.5; a very strong increase in the dissolution speed could be clearly detected at pH ~4.

The most important finding was that the dissolution proceeded just along the pre-existing edges and not on the terraces within the pH range from 5.5 to 3.8. Considering the crystallographic structure of the ZnO (Figure 6), it is quite clear why the etching process preferably proceeds at the edges of the structure. Because the point of zero charge (PZC) was evaluated to be at $pH_{PZC} = 8.7 \pm 0.2$ (Supporting Information) the Zn-terminated ZnO(0001)−Zn surface is first of all positively charged at these pH values; therefore, an attack of protons at

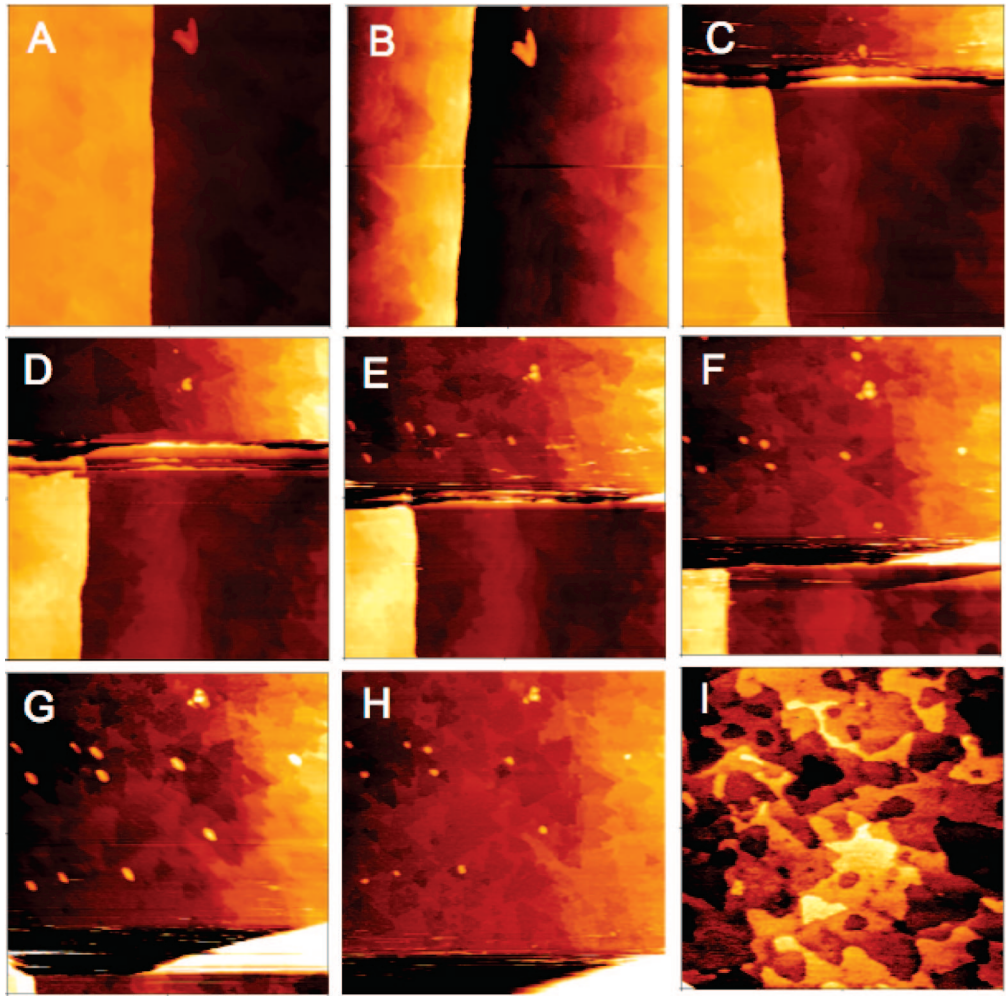

Figure 5. Evolution of the ZnO(0001)−Zn surface topography after switching the pH from 3.6 to 3.0. The scan size of the topography images was set to 1 μm × 1 μm. The images present one scan after the other from A to H, which is a period of about 25 min. In C, the final base solution pH of 3 was reached inside the cell as confirmed by measuring the fraction after the cell. The preferable etching along the edges can be seen clearly. In C−F, one can see another edge successively dissolving into the investigated area, which has a high step height of 10 nm. This high step height might be the reason that this direction appears to dissolve much faster than the other edge shown. However, it is very interesting that the structure evidently starts to show triangular features with 60° angles, which corresponds to the hexagonal surface structure. In I, a scan after switching the pH back to 6 and thereby stopping the dissolution process is shown. This structure clearly indicates atomically flat terraces and therefore crystallinity. The steps from one terrace to the other display a height of 2.5 ± 0.2 Å, which corresponds to one Zn−O double-layer step height.

these sites cannot be expected to be favorable. In contrast, the edges always present other crystallographic orientations of the single crystal (e.g., $11\bar{2}0$ or $10\bar{1}0$ could run along the steps). All of the possible edge surfaces have similar characteristics in terms of presenting oxygen at the surface as well. Oxygen atoms have one dangling bond at these surfaces. It can be assumed that the first step of the ZnO dissolution is always the reaction of a proton with a surface oxygen forming an OH^- and/or H_2O ligand to the neighboring Zn atoms. Therefore, it is quite clear that a dissolution process will preferably proceed along the edges of a Zn-terminated ZnO(0001) crystal. A reaction at the fourth tetraedric coordination position (i.e., a dangling bond) with protons from the bulk solution is favorable at these surfaces (1 in Figure 6). The adsorption of protons at the polar ZnO(0001) surface is not favorable because the surface is (a) positively charged (pH_{PZC} = 8.7 ± 0.2; Supporting Information) and (b) the oxygen atoms of the underlying layer are tetrahedrally coordinated (2 in Figure 6). This effectively inactivates the dissolution of ZnO on the polar (0001) face. Once the dissolution of a step atom occurs, further dissolution will most probably run along the freshly created kink site. However, this cannot be resolved adequately with AFM in situ.

Within a pH range of ~3.8–3.6, the dissolution started to proceed on the terraces, as clearly seen in Figure 4b−f. Nevertheless, the preferable etching sites were still the edges. When the pH was decreased further, the attacks on the terraces significantly increased the nanoroughness on the terraces, but even at pH values as low as 3, fast etching still proceeded preferably at the edges. The etching sequence in Figure 5 shows the evolution of the topography in a solution at pH 3. In Figure 5c, one can observe another edge dissolving into the investigated area of the surface, which further dissolves as displayed in Figure 5d−h.

Interestingly, it was reproducibly observed that the surfaces show crystalline features even at pH 3 (Figure 5b−i). These features cannot be found on the entire crystal but at many areas all over the crystal (see LEED discussion), which can be proven ex situ (Figure 8b) on crystals that were used for the LEED investigations as well. The structure turned out to be very different (e.g., the plateaus in Figure 5d−i show various steps): terraces with typical angles reflecting the hexagonal surface structure and a very high density of edges could be observed. Equilateral triangles were consistently found on these surfaces. The measured step heights of 2.6 ± 0.2 and 5.2 ± 0.2 Å are within the experimental error, consistent with the expected values for the

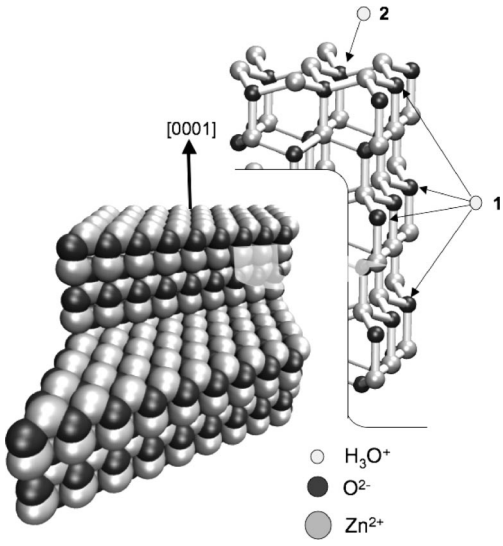

Figure 6. Perspective model of the crystallographic structure at a step and a side view of a typical low-index step surface. The [0001] surface is terminated by a hexagonal close-packed Zn layer. All possible step surfaces have surface oxygen atoms with one dangling bond. Proton adsorption at these positions (1) is clearly favorable compared to the [0001] surface (2).

ZnO crystal structure.[27] In fact, the triangular features and the high density of steps are comparable to the surface structure found for UHV-prepared surfaces. The ZnO(0001)−Zn surfaces prepared under UHV conditions are not stabilized by hydroxide adsorption but by the formation of triangular reorganization and a high density of steps.[9,10,28] Because hydroxide stabilization is not possible in highly acidic solutions, it is likely that the crystalline parts of the surface stabilize according to a similar mechanism.

DFT calculations made by Kresse et al.[28] revealed that the formation of triangular reconstructions enables the energetic stabilization of the ZnO(0001)−Zn surface in the absence of sufficient hydroxide coverage. The energy gain due to the formation of triangular features could be clearly related to the decrease in the Madelung energy. The formation of triangular structures reduces the number of repulsive next-nearest-neighbor interactions in the second coordination shell to four or five on the surface. In the proximity of isolated vacancies, the number of next-nearest neighbors would still be six. Thus, a gain of Madelung energy leads to a stabilization of triangular reorganizations rather than to the formation of isolated vacancies.

It has to be pointed out that these calculations have been performed for ZnO(0001)−Zn surfaces under UHV conditions. In electrolyte solutions, the formation of triangular reorganizations is possibly also favorable as the result of a gain of Madelung energy at these very low pH values. However, in aqueous electrolyte a gain of Madelung energy is difficult to quantify because the adsorption of oriented water dipoles has to be considered. This could lead to a much lower energy gain related to the Madelung energy. Therefore, it is reasonable to consider other possible reasons for the stability of triangular features.

Triangular features could be promoted on the basis of the delimitation by lowest-energy step-edge configurations. The triangular geometry of the nanoterraces supports this hypothesis. If one specific step orientation is most stable and thus most favorable, then it will exist on the close-packed surface within the hexagonal wurtzite structure exactly along three symmetry-equivalent directions that are rotated 120° with respect to each other (Figure 7a). Thus, the formation of equilateral triangular features indicates one specific step orientation. This conclusion can be experimentally supported if the triangular features are rotated by 60° with respect to each other on plateaus that are separated by one double layer of ZnO. The same step termination along the next Zn-terminated layer must be rotated by 60° because ZnO features an [-A-B-a-b-A-B-a-b-] structure of hexagonally close-packed planes of Zn (A/a) and O (B/b) along the *c* axis (Figure 1). Zinc planes that are separated by one ZnO double layer are rotated by 60° with respect to each other. Thus, an "A" Zn plane is rotated by 60° with respect to an "a" Zn plane; consequently, equivalent edge terminations must be rotated by 60° with respect to each other.

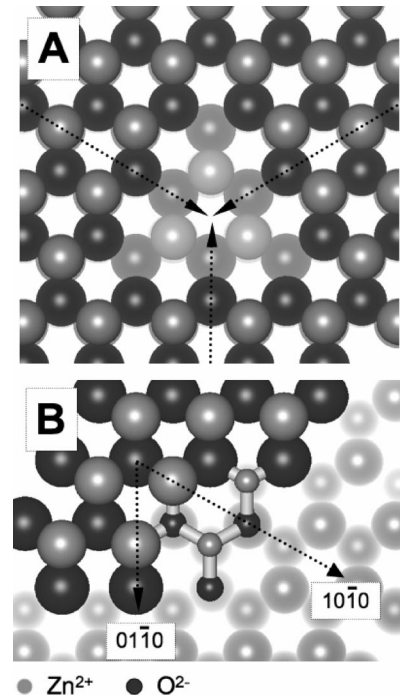

Figure 7. (A) Equilateral triangle delimited by symmetry-equivalent step orientations. Only triangular features allow termination by the same step orientation on all three sides. (B) Two possible step orientations. The $(10\bar{1}0)$ orientation yields to 3-fold-coordinated oxygen atoms at the steps. Furthermore, it is the close-packed orientation. All other possible step orientations, such as the $(01\bar{1}0)$ orientations, are delimited by, at maximum, 2-fold-coordinated oxygen atoms. If oxygen atoms were dissolved on either of the orientations, then the remaining Zn atoms would be at a maximum 2-fold coordination. Thus, the close-packed but oxygen-terminated step termination is most likely the most stable configuration.

These exact surface structures could be observed for all ZnO(0001)−Zn crystals that were immersed in electrolyte solutions with pH values lower than 4, as can be seen, for example, in Figures 5e−i and 8b. (See also ref 19.) Therefore, it can be concluded that the triangles are delimited by one specific symmetry-equivalent and most probably closed packed surface orientation.

The intriguing question is, which termination this might be. A simple evaluation based on the atomic configuration suggests that a termination with zinc atoms is not favorable even though one might argue that O-termination is unlikely in acidic electrolyte. No matter how a step edge is cut into the ZnO(0001)–Zn surface - Zn- atoms will at maximum be 2-fold coordinated (see Figure 7b). In contrast, an oxygen termination with 3-fold coordinated

(27) Reeber, R. R. *J. Appl. Phys.* **1970**, *41*, 5063–5066.
(28) Kresse, G.; Dulub, O.; Diebold, U. *Phys. Rev. B* **2003**, *68*, 016102-1–016102-4.

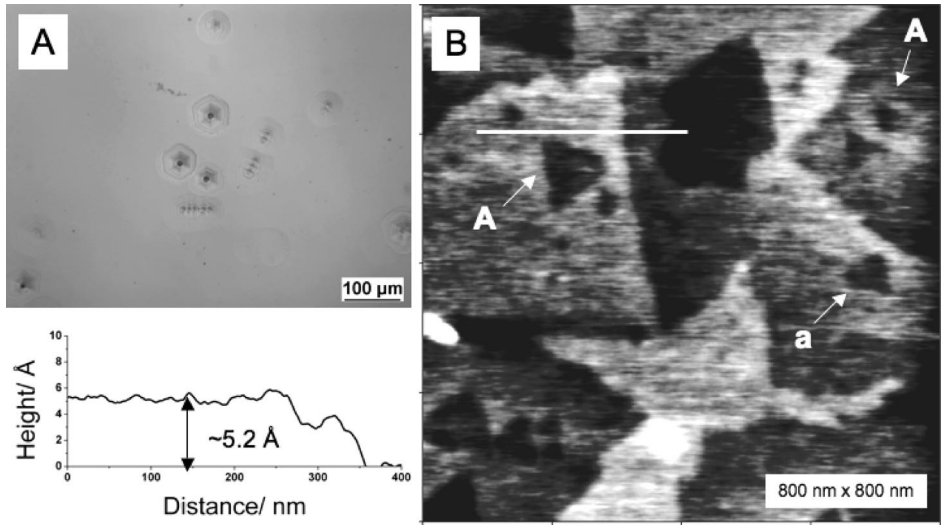

Figure 8. (A) Photomicrograph of the surface after etching in a solution at pH 3. Hexagonal etching pits can be clearly seen. (B) Ex-situ AFM topography scan on a surface between the etching pits. Triangular features on the surface are clearly visible, and crystallinity is evident. As can be clearly seen, triangular features on "A" terraces are rotated 60° with respect to triangles on "a" terraces. The line profile (measured as indicated) shows that the step heights correspond to the expected Zn−O double-layer height.

oxygen atoms is possible along the closed packed $(10\bar{1}0)$ direction. To explain this unexpected stability of oxygen terminated step edges at low pH we assume a proton adsorption at the dangling bond of oxygen but dissolution could still be kinetically effectively inhibited for such a configuration. This would suggest that dissolution is much more favorable at kink-site positions. Consequently triangular pits - which do not feature kink-sites - are quite stable. As the triangles also grow with increasing time of exposure it must be possible to dissolve step atoms as well. Therefore we assume that the surface structure sufficiently stabilizes due to the formation of triangular features in electrolyte solutions even though they are oxygen terminated. Moreover this indicates that the dissolution mechanism not only runs along surface orientations that present oxygen atoms but preferably proceeds via kink-sites as well, as it was also concluded from the electrochemical dissolution experiments by H. Gerischer et al.[12,13]

To conclude it is not possible to decide which of the discussed effects finally leads to a stabilization of the crystalline triangular features. Most probably it is an interplay of both discussed effects, i.e. a stabilization (1) due to a gain of Madelung energy and (2) due to the formation of oxygen-terminated $(10\bar{1}0)$-orientated step edges within the acidic environment. However, further investigations are necessary to finally decide on the termination because -so far not considered - atomic relaxations at the step edge could also favor some other step-orientation.

The results of the AFM dissolution studies can be summarized as follows:

(1) The surface topography turned out to be stable within the investigated time scale between pH 11 to pH 5.5.

(2) The dissolution starts at pH 5.5 and proceeds preferably along the edges and most favorable along kink-sides at all pH values.

(3) Below pH 3.8 the ZnO(0001)–Zn terraces become unstable because hydroxide stabilization is not effective anymore; i.e. the very strong (covalent) bonding[28] of surface hydroxides is broken by protonation from the bulk solution. Consequently, a new mechanism leading to the formation of triangular structures stabilizes the crystalline Zn-terminated surface at low pH values.

Stability and Dissolution on ZnO(0001)−Zn Surfaces: Ex-Situ LEED Studies Complementary to the AFM studies, LEED investigations were performed with equally prepared surfaces to prove that the surfaces consist of a well-ordered crystalline structure on terraces within electrolyte solutions. Therefore, the surfaces were treated with the same electrolyte solutions as used for the AFM studies according to the following protocol.

After preparation, the surfaces were immersed in Ar-purged electrolyte solution of a certain pH value (starting at pH 11) for 10 min, rinsed with ultrapure water (pH usually between 6.0 and 8.0, no dissolution), dried in a stream of nitrogen, and directly introduced into the UHV system for the LEED analysis. Practically, the sample transfer from the solution to the UHV chamber took about 3 min. This time was short enough to avoid surface contamination. After the LEED measurement, the surfaces were taken out of the UHV system again, and the same procedure was repeated at a lower pH value. As can be seen in Figure 8, the surfaces led to sharp LEED patterns at electron energies from 20 eV up to 112 eV, suggesting a well-defined crystalline structure at the surface. The characteristics of LEED patterns did not change if the surfaces were treated with solutions within a pH range of 11.0 to 4.0. Representative LEED patterns are depicted in Figure 9(a−c). In comparison with the AFM investigations, this behavior clearly reveals that the surface structure, precisely, the structure on the terraces, is well-ordered, crystalline, and stable in electrolytes within this pH range. Below pH 4, the LEED characteristics of the surfaces changed significantly; however, it was always possible to obtain sharp LEED patterns of surfaces that were treated with electrolytes with pH values lower than pH 4 (Figure 9d,e). The observed changes can be described as follows.

First, a shifting of the surface under the LEED beam reveals that there were areas where the patterns are weaker and areas were the patterns were sharp. It can be concluded that the analyzed surface consisted of crystalline and amorphous areas. LEED, as an integral technique, leads to patterns when the crystalline surface area of the crystal is above a certain critical value. However, if ZnO(0001)−Zn surfaces were etched at pH values below 3.8 the surface topography was partly ill defined. An inspection of the surfaces with the optical microscope showed that a lot of hexagonal etching pits were formed (Figure 8a). In between these defects, crystalline areas could be observed by means of AFM (8b). It is well known that the formation of hexagonal

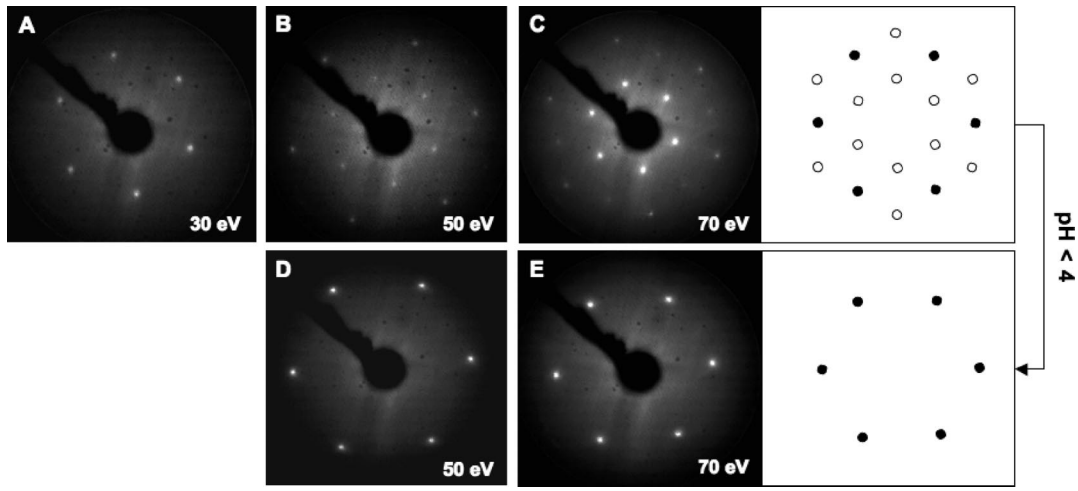

Figure 9. (A−C) Characteristic LEED patterns of the ZnO(0001)−Zn surfaces after immersing into solutions of different pH values from 11 to 4. They clearly indicate a well-ordered crystalline structure on the terraces for all pH levels. (D, E) Characteristic patterns after immersing the surfaces into solution with pH <4.0. The LEED characteristics of the surface changed significantly. First, the lower-energy patterns at 20–30 eV could not be observed anymore. Second, it can be seen clearly that also at 50 and 70 eV specific patterns disappear as shown in the schematics of the 70 eV patterns as well. This clearly indicates a superstructure that is irreversibly destroyed by immersion of the surface at pH values lower than 4.0. A $\sqrt{3}\cdot\sqrt{3}$·R30 superstructure of hydroxides on the surface that is bound very strongly to the surface can explain this structure.

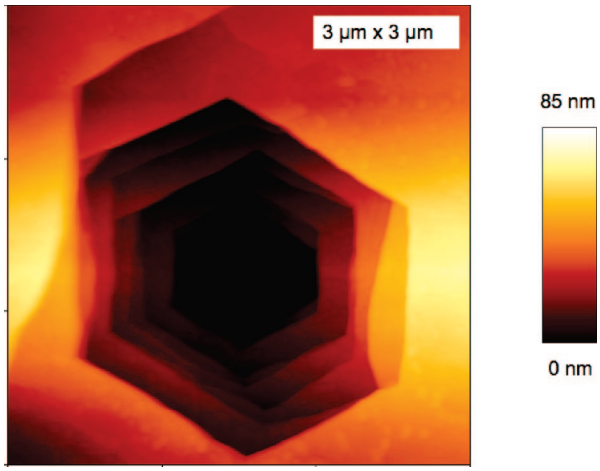

Figure 10. Typical AFM topography image of a hexagonal etching pit.

etching pits is specific to the ZnO(0001)−Zn surface.[29] Considering the etching mechanism as discussed above, it is quite clear that this surface orientation exhibits such etching pits. Obviously, the etching process can start at certain positions such as surface defects with a vertical attack into the bulk oxide. Subsequently, the etching proceeds again perpendicular to the direction of the polar plane as can be seen in the AFM topography of a pit (Figure 10). Dislocations of the crystal could serve as nucleation sites for such defects. Furthermore, the occurrence of these hexagonal etching pits clearly indicates that the different edge surface orientations must have approximately the same dissolution kinetics.

Second, some of the LEED patterns disappeared after immersion of the surface into electrolyte solutions at pH values lower than pH 4. This was especially obvious for the patterns at energies lower than 40 eV, which disappeared, as can be seen in Figure 7(d,e). A further inspection of the LEED patterns revealed that certain patterns disappear at all electron energies for pH values below 4. In return, patterns that have been weaker for surfaces immersed at higher pH values became clearly visible after immersion in solutions with pH values lower than 4, as can be seen in the comparison presented in Figure 9.

Therefore, the loss of patterns can be interpreted as the loss of a well-ordered hydroxide superstructure. This indicates that the ordered hydroxide superstructure was destroyed by immersion in electrolytes with pH values below 4. The patterns that are clearly visible at low pH values are the [1 × 1] patterns of the ZnO(0001)−Zn substrate that are much more intensive after destruction of the superstructure ad-layer. The lost patterns can be assigned to a $\sqrt{3}\cdot\sqrt{3}$·R30 superstructure of hydroxides. According to earlier investigations with angle-resolved XPS and ToF-SIMS, the as-prepared ZnO(0001)−Zn surfaces, which also show these low-energy patterns, are hydroxide-terminated.[18]

Consequently, at pH values below 4 the well-ordered structure of hydroxides is attacked and irreversibly destroyed. This leads to a destabilization of the surface as the AFM measurements indicated. Nevertheless, the patterns of the [1 × 1] ZnO(0001)−Zn surface are still very sharp and intensive, which rules out an amorphous layer as well. At pH values below 4, the surface is Zn-terminated and single-crystalline. An $E-V$ curve would possibly reveal a broadening of the spots due to the formation of a much more dense step-and-terrace structure.[30] However, on the basis of the presented LEED pictures this cannot be seen clearly. To conclude, the LEED investigations support the AFM results and suggest that the hydroxide-stabilized surface is destabilized as a result of the high proton concentration and is then restabilized as a result of the formation of triangular reorganizations, which are Zn-terminated on the terraces and thus show [1 × 1] LEED patterns.

On the basis of these findings, it can be clearly argued why dissolution can also start to proceed on terraces below pH ∼3.8, as was seen in the AFM measurements. It can be concluded that the surface structure on the plateaus is not sufficiently stabilized by hydroxides at these acidic pH values. The obviously very stable hydroxide coverage is dissolved at these low pH values as a result of protonation of the surface hydroxides. The surface energy will be quite high because of these unfavorable conditions. Consequently, the reaction of a proton with an oxygen atom from one atomic layer below the Zn layer will be favorable

(29) Mariano, A. N.; Hanneman, R. E. *J. Appl. Phys.* **1963**, *34*, 384–388.

(30) Henzler, M. *Appl. Surf. Sci.* **1982**, *11–2*, 450–469.

because it will weaken the bond to the surface Zn ions and thereby promote the Zn ion dissolution to the bulk solution. Hence, an energetically more stable situation will be promoted. Once such a defect is created, the dissolution will proceed along such a defect as far as kinetically inhibited and energetically favorable triangular structures form and sufficiently stabilize the surface in acidic environment.

Summary and Conclusions

By means of in situ AFM and ex-situ LEED studies, it was proven, that the hydroxide stabilized ZnO(0001)–Zn surface is stable in electrolytes within a pH range from 11 to 5.5. The stability of the single-crystalline ZnO(0001)–Zn surface in aqueous electrolytes was found to be based on hydroxide adsorption as an efficient stabilization mechanism for polar surfaces in electrolytes. Such a stabilization mechanism is well-known e.g. for CuO(001) and NiO(111) surfaces as well.[31,32] It is not yet clear if this is generally valid for all polar surfaces in aqueous electrolytes. However, we think there is strong evidence that this could be a general phenomenon of polar tasker-type 3 surfaces.

It was further shown, that an imaging of the topography of the ZnO allows conclusions on the dissolution mechanism of ZnO(0001)–Zn surfaces. Below pH 5.5 dissolution of the ZnO surface starts with a very slow rate. The in situ AFM studies show, that this dissolution proceeds preferably along the pre-existing edges of the crystalline surface structure; the ZnO(0001)–Zn terraces are still intact and feature a well-ordered $\sqrt{3}\cdot\sqrt{3}\cdot R30$ hydroxide super structure until a certain level of proton-concentration is reached as could be shown by the ex-situ LEED studies. This preferential dissolution can be interpreted in context with the crystallographic features of the respective etching sites. As a first step of an acidic dissolution the reaction of a proton with an oxygen-ion can be expected. Therefore, etching of the crystal proceeds preferably from crystallographic surface orientations where oxygen ions are present. The structural precondition for ZnO dissolution is the existence of a dangling bond of an oxygen ion at the oxide/water interface, which acts as an adsorption site for protons. This situation is prevalent on the edges but not on the hydroxide stabilized faces of the ZnO(0001)–Zn surface. Consequently, the terraces are inert with regard to the protonation reaction and dissolution preferentially proceeds along step edges.

However, below pH ~3.8 dissolution events can occur on the ZnO(0001)–Zn terraces as well, which was discussed in terms of a destabilization of the surface structure. Both, the in situ AFM and the ex-situ LEED investigations support the assumption that hydroxide stabilization is effectively destroyed at pH values below 3.8. Surface destabilization due to the dissolution of the well-ordered surface hydroxides and restabilization via formation of triangular reorganizations were observed at pH values below 3.8. The ZnO(0001)–Zn surface changes its stabilization mechanism below this pH value due to first the minimization of the Madelung energy and second the preferable formation of stable $(10\bar{1}0)$ step orientations by the evolution of triangular reorganizations. In fact this is a very interesting result, because this is according to the best of our knowledge the first in situ observation of a change of the stabilization mechanism of a polar oxide surface. Finally, it could be shown that - after reorganization of the surface structure toward triangular reorganizations - etching further proceeds preferably along the edges at these highly acidic pH values below pH 3.8.

Acknowledgment. The financial support of voestalpine Stahl Linz GmbH, Henkel Surface Technologies, and the Christian-Doppler Society in Vienna is gratefully acknowledged. S. Borodin acknowledges IMPRS Surmat for financial support through a fellowship. Furthermore, we thank Dr. M. Rohwerder for helpful discussions concerning the LEED experiments.

Supporting Information Available: Measurements of the point of zero charge (PZC) based on Chemical Force Spectroscopy by means of AFM are presented. This information is availabe free of charge via the Internet at http://pubs.acs.org.

LA7037697

(31) Zuili, D.; Maurice, V.; Marcus, P. *J. Electrochem. Soc.* **2000**, *147*, 1393–1400.

(32) Kitakatsu, N.; Maurice, V.; Hinnen, C.; Marcus, P. *Surf. Sci.* **1998**, *407*, 36–58.